Science of the Total Environment 533 (2015) 8–16

Contents lists available at ScienceDirect

Science of the Total Environment

journal homepage: www.elsevier.com/locate/scitotenv

The effect of ego-motion on environmental monitoring

Uri Lerner [a,b], Tamar Yacobi [a,b], Ilan Levy [b], Sharon A. Moltchanov [a,b], Tom Cole-Hunter [c,d,e], Barak Fishbain [a,b,*]

[a] Technion Enviromatics Lab. (TechEL), Dept. of Environmental, Water and Agricultural Engineering, Faculty of Civil & Environmental Engineering, The Technion — Israel Institute of Technology, Israel
[b] Technion Center of Excellence in Exposure Science and Environmental Health (TCEEH), Dept. of Environmental, Water and Agricultural Engineering, Faculty of Civil & Environmental Engineering, The Technion — Israel Institute of Technology, Israel
[c] Centre for Research in Environmental Epidemiology (CREAL), Barcelona, Spain
[d] Centro de Investigación Biomédica en Red de Epidemiología y Salud Pública (CIBERESP), Madrid, Spain
[e] Universitat Pompeu Fabra (UPF), Barcelona, Spain

HIGHLIGHTS

- First assessment of the impact of air pollution micro-sensing units' ego-motion on their accuracy in mobile application.
- Evaluation is done through lab experiments and a field campaign.
- Means to cope with ego-motion associated bias are suggested.
- These suggestions present a valuable tool to improve environmental monitoring using MSUs in general or by mobile deployment.

GRAPHICAL ABSTRACT

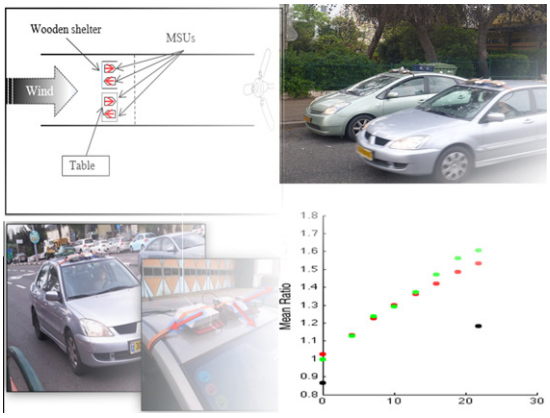

ARTICLE INFO

Article history:
Received 30 April 2015
Accepted 17 June 2015
Available online 4 July 2015

Editor: D. Barcelo

Keywords:
Air pollution
Exposure
Monitoring
Micro sensing units
Ego-motion
Micro-Sensor Calibration

ABSTRACT

Air pollution has a proven impact on public health. Currently, pollutant levels are obtained by high-priced, sizeable, stationary Air Quality Monitoring (AQM) stations. Recent developments in sensory and communication technologies have made relatively low-cost, micro-sensing units (MSUs) feasible. Their lower power consumption and small size enable mobile sensing, deploying single or multiple units simultaneously. Recent studies have reported on measurements acquired by mobile MSUs, mounted on cars, bicycles and pedestrians. While these modes of transportation inherently present different velocity and acceleration regimes, the effect of the sensors' varying movement characteristics have not been previously accounted for.

This research assesses the impact of sensor's motion on its functionality through laboratory measurements and a field campaign. The laboratory setup consists of a wind tunnel to assess the effect of air flow on the measurements of nitrogen dioxide and ozone at different velocities in a controlled environment, while the field campaign is based on three cars mounted with MSUs, measuring pollutants and environmental variables at different traveling speeds. In both experimental designs we can regard the MSUs as a moving object in the environment, i.e. having a distinct ego-motion.

* Corresponding author at: Technion Enviromatics Lab. (TechEL), Dept. of Environmental, Water and Agricultural Engineering, Faculty of Civil & Environmental Engineering, The Technion — Israel Institute of Technology, Israel.
E-mail address: fishbain@technion.ac.il (B. Fishbain).

http://dx.doi.org/10.1016/j.scitotenv.2015.06.066

The results show that MSU's behavior is highly affected by variation in speed and sensor placement with respect to direction of movement, mainly due to the physical properties of installed sensors. This strongly suggests that any future design of MSU must account for the speed effect from the design stage all the way through deployment and results analysis. This is the first report examining the influence of airflow variations on MSU's ability to accurately measure pollutant levels.

1. Introduction

Exposure to air pollution is recognized as a contributing factor for various physiological effects and associated risks to public health (International Agency for Research on Cancer (IARC), 2013). The study of air pollution and its exact effects calls for accurate exposure assessments. Air pollution related exposure metrics, typically used in environmental epidemiology studies, are based either on (1) short term surveys using a large number of sensing devices over a short period of time to obtain a high-resolution spatial pollution image (e.g. Crouse et al., 2009); or (2) air pollution measurements acquired from standard Air Quality Monitoring (AQM) stations over extended time periods (e.g. Pope et al., 2002). AQM stations do provide accurate measurements but are large, expensive and require skilled personnel for routine maintenance. Thus, they are few in number and therefore lack the ability to account for the spatial variability of pollution levels in heterogeneous regions (such as urban areas), rendering exposure assessment a very difficult task (Rao et al., 2012).

In an attempt to cope with the isolated nature of the measurements taken by AQM networks, different modeling approaches are used to expand the localized results into high-resolution exposure maps, such as ordinary kriging (Whitworth et al., 2011), or inverse distance weighting and land use regression (Levy et al., 2015). However, these models are more suitable for long-term, chronic exposure studies, due to their aggregative nature, and the possible loss of short-term localized measurements needed for more acute exposure incidents (Karr et al., 2009; Brauer, 2010). A better solution may be to use a denser array of sensing nodes, and thus create a better interpolation, closer to the real-life pollution dispersion scenario (Kanaroglou et al., 2005).

Recent developments in sensory and communication technologies have made the development of small, portable and relatively low-cost sensing units possible. These micro sensing units (MSUs) can be used as a set of individual nodes, interconnected to construct a Wireless Distributed Environmental Sensor Network (WDESN), aimed at measuring air pollution as one unit, gathering high-resolution spatial and temporal data.

Initial studies testing the feasibility of such MSUs in pre-field and field trials showed that these units indeed capture air pollution spatio-temporal variations. Their downfall, however, is their relatively low accuracy compared to AQMs or other benchmark devices (Lee and Lee, 2001; Becker et al., 2000; Mead et al., 2013; Williams et al., 2013; Molchanov et al., 2015). Studies that evaluated MSUs' capabilities in a controlled lab environment emphasized the need for a calibration process (Lee and Lee, 2001; Becker et al., 2000). Field deployments of low-cost air quality sensor networks measuring ambient O_3 levels by metal-oxide microsensors (Williams et al., 2013) and CO, NO and NO_2 by electro-chemical (Mead et al., 2013) or metal-oxide (Piedrahita et al., 2014) probes proposed calibration processes that are applicable to a controlled lab environment but fall short in comparison to data collected at a collocated standard AQM station, even after an initial field calibration had been applied (Williams et al., 2013). Molchanov et al. presented an in-field calibration process (Molchanov et al., 2015), however their calibration procedure strongly relies on the sensors being stationary. Tsujita et al. (2005) suggested a field calibration approach where the metal-oxide NO_2 sensor baseline is adjusted to the average value of four surrounding AQM stations during time periods in which the NO_2 concentrations are low ($\ll$10 ppb) and homogeneous meteorological conditions apply. Yet, the method is designed to work with low NO_2 concentrations whereas the MSUs' NO_2 detection limit is typically at or above such low concentrations (10 ppb). This renders the method inapplicable. Spinelle et al. suggested a protocol for evaluation and calibration of low-cost gas sensors (Spinelle et al., 2013), reemphasizing the need to account for the wind conditions that the sensors are expected to work under. Thus, it was acknowledged that wind does have an effect on the measurements, however their protocol does not quantify the nature of this effect.

The small size and low power-consumption of MSUs also allow for mobile measurements. Placing these units on mobile platforms enables the coverage of a wider area with a smaller number of units, while keeping the spatial and temporal resolution high. Few recent studies showed the possibility and advantages of such use, and the relatively easy adaptation of such MSUs to function as mobile sensing units, with the addition of GPS (Al Ali et al., 2010; Devarakonda et al., 2013). These studies based their design on the assumption that mobility itself has no effect on the sensors' functionality. An attempt to consider this issue was done by Levy et al. (2014) in a mobile field-experiment in an urban environment in Montreal, Canada. Their study showed that a correction has to be applied to particulate matter measurements taken while moving, due to the varying flow rate effect on the collection efficiency of the instrument. However, they didn't regard gas-phase pollutants in this correction since the gas measuring instruments had a regulated flow rate, i.e., active sampling, and the sensing apparatus was standard AQM measurement equipment, rather than low-cost, diffusion-only-based gas sensors, i.e. passive sampling.

The gas sensors installed on the Elm™ units used in this study are passive metal-oxide sensors (MOS). When the sensor faces the winds' inflow direction, an increased flow is created on the sensors' face, affecting its behavior (Honicky, 2011). The effect is due to the metal-oxide sensors having a preliminary heating phase of ~300 °C designed to evaporate the sampled air and initiate the proper reaction conditions on the MOS surface. A shift in the surface temperature caused by the increased air flow can divert the sensor from its calibrated status and alter its output. Wang et al. (2010) showed that metal-oxide gas sensors are sensitive both to ambient temperature as well as relative humidity (RH), as later shown, two variables that have been found to be affected by the traveling speed.

As such, this paper focuses on the use of MSUs for urban air-quality monitoring, by means of mobile deployment. The aim was to test the validity of measurements made by sensors traveling at different velocities, through comparing mobile and stationary measurements taken at the same time and location. To this end, laboratory work and a field campaign were performed.

2. Materials and methods

2.1. Sensing equipment

All air quality measurements were taken using Elm™ MSUs (PerkinElmer LTD, USA (PerkinElmer)). Each Elm™ unit is encased in a relatively-small weather-resistant metallic case (sizing 26 × 17 × 7 cm, L W H), and consists of two semiconducting MOS (measuring O_3 and NO_2). Each sensor has an 18 mm inlet which is significantly larger than the sensors' sensing face, electret microphone for noise level measurements and dual semiconductor temperature and RH sensor (See Table S1, in the supporting information, for detailed sensor

specifications). In this study the above environmental variables were analyzed for stationary and mobile configurations at the same micro-environment. The comparison of the mobile and stationary sensors under the same environmental conditions facilitates assessment of ego-motion effect on the measurement. The sensors are installed so that they face different sides of the unit casing as described in Fig. 1(a). Measurements are computed as averaged readings at varying intervals for the different variables (Table S1 in the supplementary material), and transmitted to a cloud-based storage by an on-board GSM-embedded chip.

2.2. Laboratory setup

2.2.1. Experimental design

Four Elm™ units were placed inside a wind tunnel, 250 cm away from the tunnel's inlet, and 71 cm above the floor (Fig. 1b). The four units were placed adjacent to each other, at the same height, with no more than 30 cm between all sensors' inlets.

Two units in the wind tunnel were exposed (E) to the flow, while the other two were covered behind a wooden barrier (C), rising 40 cm above the units (i.e. 111 cm above the floor), and covering their entire length from the wind. Of each unit couple, one was facing the incoming flow (i.e. forward-facing (F), see Fig. 1b), and the other faced the opposite direction (backward-facing (B)). Thus the four units are marked as forward-exposed (F-E), forward-covered (F-C), backward-exposed (B-E) and backward-covered (B-C). All measurements were performed at ambient concentrations of the various pollutants without any artificial introduction of substances to the wind tunnel. The wind flow in the tunnel is computer-controlled, calibrated to generate specific wind velocities in a laminar regime (turbulence levels under 5%). The ambient levels inside the wind tunnel (when idle, i.e. wind speed is zero) for NO_2, O_3, RH, Temperature and Noise are 83 ppb, 30 ppb, 76%, 26 °C and 66 dB, respectively.

Three separate trials were conducted. The first two consisted of a pyramid-like variation in wind velocities, increasing from 0 km/h to the tunnel's maximum air flow speed of 22 km/h, and decreasing back to 0 km/h at stages of speeds (Fig. S1a in the Supplementary material). Higher wind speeds were measured during the field campaign described next. During the third trial the velocity was altered directly between the minimum (0 km/h) and maximum (22 km/h) speeds, repeating the process three times (Fig. S1b). For all three trials, each different velocity was held for a period of 10 min. The results were analyzed both by measured values and by comparison between sensor pairs (e.g. F-E vs. F-C, or F-E vs. B-E). The ratio between the E sensor's and the C sensor's concurrent readings is evaluated for assessing the wind speed effect. As a sensor's surface temperature is linear with respect to wind speed (Wooten, 2011) and a sensor's measurements are linearly-dependent on a sensor's surface temperature (Wang et al., 2010), this ratio of E vs. C sensor measurements is also expected to be linear with respect to wind speed as well. This analysis was repeated for all environmental variables measured by the ELM™ units (i.e., noise, temperature, RH, NO_2 and O_3).

2.2.2. Calibration process

Following Molchanov et al. (2015), initially all sensors were placed together in the wind tunnel in order to obtain a common base line (Molchanov et al., 2015). In this process, for each environmental variable, the sensors were calibrated to the average level of all sensors, so that in idle wind conditions (i.e. wind speed equals 0 km/h) all sensors presented the same values. During data analysis, each time throughout the lab experiment that the wind tunnel was idle, the calibration parameters were tested to check for the validity of the calibration by repeating the regression and comparing the results ($p < 0.001$).

2.3. Field campaign

2.3.1. Field study design

The field study was performed at Neve Sha'anan, a residential neighborhood in the city of Haifa, located on a relatively leveled region of the Carmel Ridge, about 200 m Above Sea Level. The neighborhood is roughly divided by a major road (Trumpeldor Ave.), which also serves as the main commercial center for the residents of this area (see Fig. 1c and Section S3 in the Supplementary material).

Nine Elm™ MSUs in total were placed on the roof of three cars, three MSUs per vehicle. As the sensors on each MSU face different sides (see Fig. 1a), the units were placed facing the front, left and right sides of the vehicle. This way each sensor composing the MSU faced the traveling direction in one MSU. Each MSU is tagged by the direction it is facing (left, right or forward) and the ID number of the car it was mounted on (1, 2 or 3). Thus, for example, the left-facing unit mounted on car

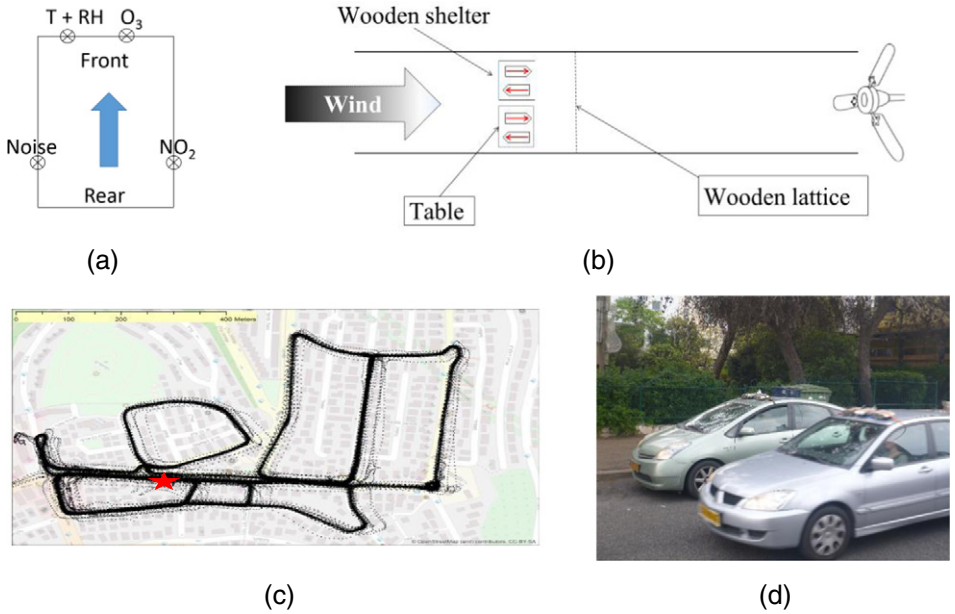

Fig. 1. Experimental setups. (a) Elm air-quality micro sensing unit (MSU) — sensing probes layout; (b) wind tunnel setup, top view; (c) field campaign design. The star marks the parked (stationary) car's position along the route; (d) driven car passing by the stationary one.

number 2 and the forward facing unit on car 3 are L-2 and F-3, respectively. In addition to the MSUs, each car was equipped with a GPS recorder (LG-Nexus 4, Avago ALM3012 chip with 10 m accuracy), and a forward-facing still camera, capturing a photo every 60 s.

For the field campaign, data from the MSUs and GPS data were organized as a 1 Hz time series for the entire trial length. To complete the time series to a 1 Hz resolution, and based on the MSU's sampling mechanism (Table S1), customized backward-interpolation was designed based on the Nearest Neighbor method, completing the gap with the averaged result for any given missing period (Junninen et al., 2004) (i.e. O_3 measurement stored in second 60 was used to complete seconds 1 through 59, and so forth).

The study was held during a regular work day, for a 10-hour period from 6:00 AM (before the morning rush-hour, 07:00–09:00 AM) to 04:00 PM (prior to the evening rush-hour, 05:00–08:00 PM). The three cars were driven on a pre-determined route (Fig. 1c) of 6.5 km and approximately 15 minutes long, passing through both heavy and low-traffic roads, at varying speeds, ranging 5–60 km/h. At any given moment, one of the three cars (interchanging) was parked with its engine turned off along the curb at a specific location on the route at Trumpledor Ave., a 2-lane street with varying traffic loads throughout the day, consisting of both private cars and buses. This location allows the development of relatively higher speeds, which results in a larger range of velocities.

To explore the effect of travel speed, the mobile car's sensors' output was compared with that of the stationary one, at the moment the moving car passed by the stationary one, chosen by proximity, as verified by GPS coordinates (Fig. 1c and d). A total of 161 passes of the traveling cars by the parked car occurred during the campaign, resulting in 483 comparisons between MSUs (3 MSUs per car). One-second measurements were used for each comparison. Comparisons were held for all unit pairs facing the same direction to avoid the possible effect of sensors' direction on the mobile vs. stationary computed ratio.

2.3.2. Traffic volumes assessment

Using photos taken by the moving car in real-time, four types of traffic loads were defined based on proximity of the nearest traveling car to the sensor-equipped vehicles, as illustrated in Fig. S3. In all four defined categories, the stationary car (S) and the moving car (M) are at the same location along the path (S — parking, M — lane 2). To define the different configurations, we used a distance threshold (d) of 15 m between car M and the nearest vehicle (N_i), if one is present. Also, the lane in which vehicle N_i was located was considered a contributing factor. Four configurations were defined: (1) N is located at the same lane as M ($d < 15$ m), with no consideration to the adjacent lane; (2) N_1 in the same lane as M ($d > 15$ m) and/or N_2 in the adjacent lane ($d < 15$ m); (3) N in the adjacent lane to M ($d > 15$ m) and (4) no nearest vehicle is present. The distance threshold ($d = 15$ m) was determined based on the location of vehicle M, with an easy to measure curbside of this length, noticeable in the available photos. Also, speed limit on this location is 50 km/h (or about 14 m/s), so the given threshold represents the time a car will pass in approximately one second, the same time-frame used for comparison of measurements, and thus it differentiates well a "close by" vs. "further away" vehicles. If no image is available (due to the frequency images are taken by the camera), configuration is referred to as (0).

3. Results and discussion

3.1. Laboratory experiment

The trials conducted in the wind-tunnel were aimed at quantifying the effect of wind velocity in a controlled environment, with no local emission sources (e.g. traffic).

At zero wind speed and under wind conditions, when all MSUs were unshielded (exposed), the sensors presented similar measurements of the ambient environmental measured variables, including the measured pollutants (O_3 and NO_2). When one of the sensors was shielded it produced the same measurements as the unshielded sensors at zero wind conditions. These examinations, and the close proximity of the sensors, suggest that all sensors are subjected to the same conditions at zero wind speed so that the only effect at play (which is different under wind conditions) is due to the wind itself.

Fig. 2 shows the correlation between all MSUs during the laboratory trials, for NO_2 and O_3. Fig. 3 shows the measurements of NO_2 (only) by all four sensors: (a) presents NO_2 levels throughout the pyramid wind pattern; (b) depicts NO_2 levels through the direct min–max alternating wind speed pattern; and (c) presents the NO_2 measured levels clustered by wind speeds. The correlation coefficient between all four sensors was high (correlation coefficient > 0.65, Fig. 2a) in all three trials. All units measured high values of NO_2 when the wind speed was 0 (i.e. measurement of ambient concentrations), reaching over 200 ppb with mean values greater than 60 ppb (Fig. 3a). These high values may be a result of the wind tunnel's location, placed between two large parking lots, where NO_2 concentrations are expected to rise during working hours (when the trial took place). Moreover, another explanation might be that these measurements might arise due to cross-interference to the NO_2 sensor by a different, unknown atmospheric component. Nonetheless, even if a potential interfering factor is involved, we still observed a change of measurements when the tunnel was activated and the wind speed increased, when all sensors converged to lower values of NO_2, close to the lower limit of measurement sensitivity (10 ppb). This phenomenon was observed at the interval trial (Fig. 3b), where at every iteration, the sensors showed high and varied NO_2 levels with no wind, but when the flow began, a sharp decrease was clearly observed. About 90 s after the wind speed decreased back to 0 km/h, the measured NO_2 values rose again, to similar levels of idle conditions. The cause for this behavior is not yet known, and requires further study. However, following the assumption that a shift in sensor temperature does occur under varying airflow conditions, a short delay before

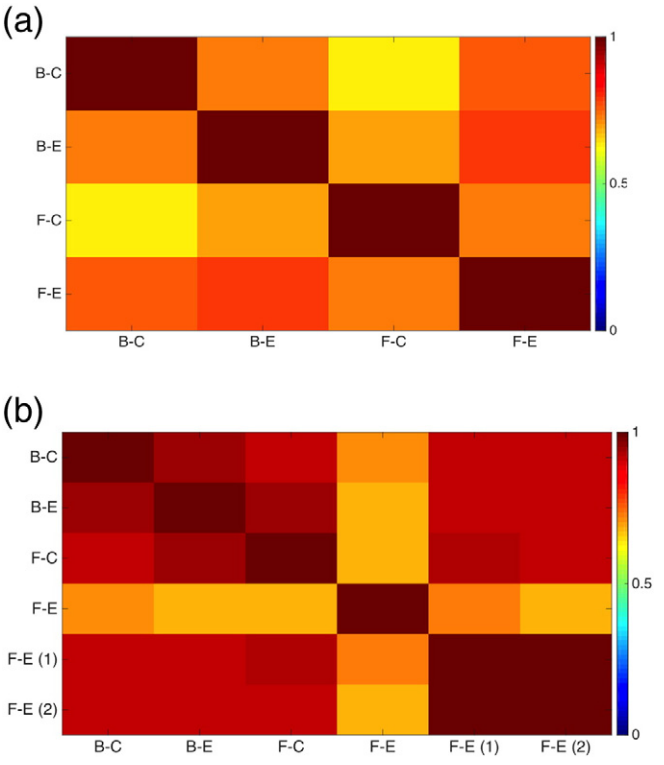

Fig. 2. Correlation plots (Pearson's r) for NO_2 (a) and O_3 (b) during laboratory trial. For O_3, correlation is displayed for the initial results and post calibration, both by F-E vs. F-C (F-E (1)) and by F-E vs. B-E (F-E (2)).

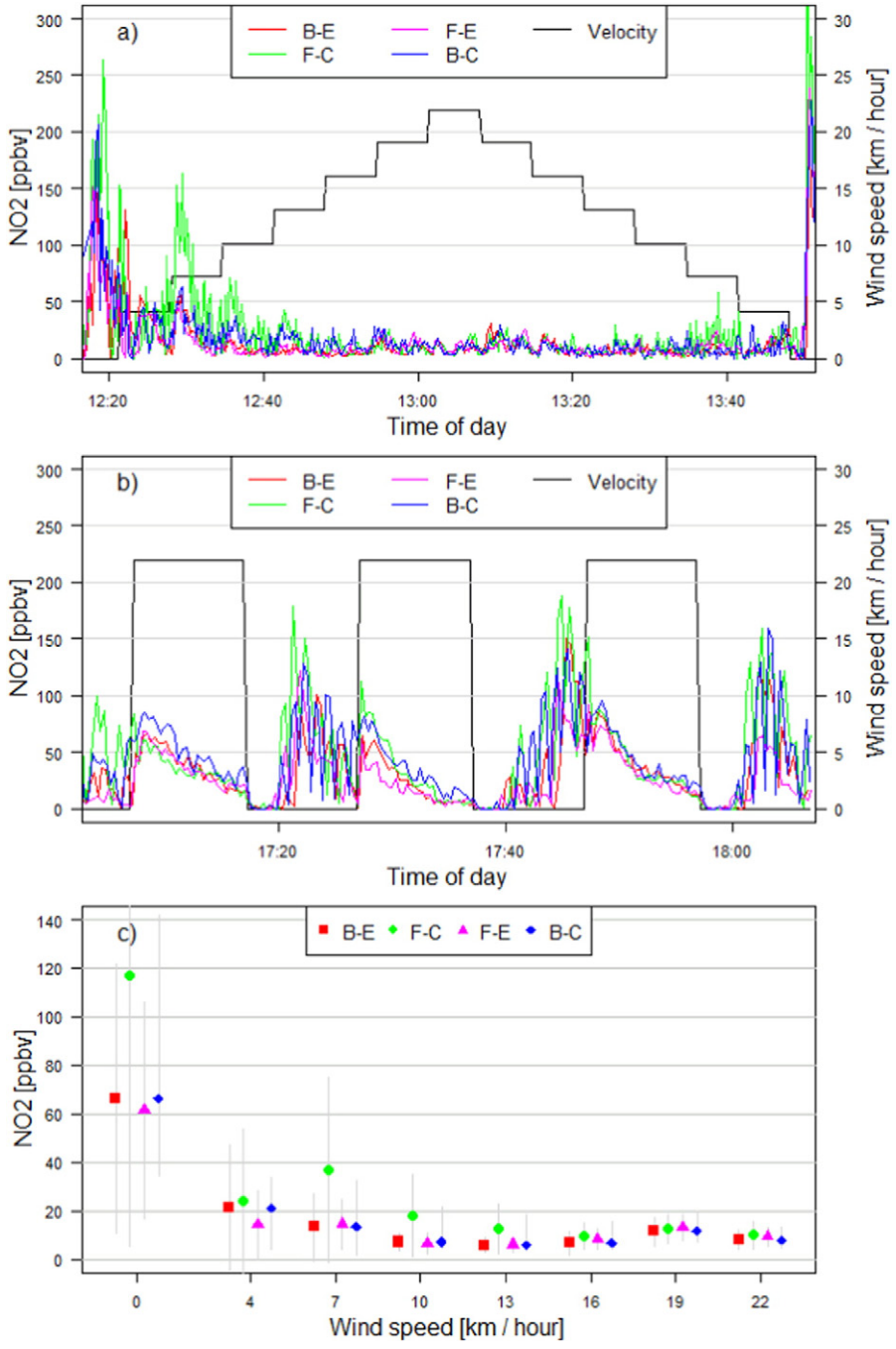

Fig. 3. Wind tunnel results — NO_2 measurements (in [ppb]) during wind-tunnel trials — (a) pyramid wind pattern; (b) alternating stop-max wind pattern. Wind speed changes are illustrated by the black line; (c) mean value of NO_2 measurements, clustered by wind velocity. B-C – blue diamond; B-E — red square; F-C — green circle; F-E — pink triangle.

the sensor resumes proper functioning is expected, as the sensor warms up back to its calibrated working conditions. This possible cause does not rely on the actual pollutant being measured by the MSU, either NO_2 or an unknown subject. Furthermore, it is noticeable that the higher the wind velocity is, the lower is the variance of the measurements. This heteroscedasticity of the samples is highly significant for all sensors, during both pyramid trials (verified using Bartlett's test for homogeneity of variance (Snedecor and Cochran, 1989), which was significant at $p \ll 0.0001$).

Fig. 3c presents apparent changes of absolute measurements with respect to wind speed. Exponential correlations were found with R^2 values of 0.77 and 0.67 for the backward and forward *exposed* MSUs (B-E and F-E), respectively. When the sensor is covered and consequentially the wind's effect is expected to be smaller, R^2 values of 0.56 and 0.39 for the *covered* forward and backward facing units (F-C and B-C, respectively) were observed. Thus, wind at the sensor's face (affecting the *exposed* MSUs) was found to play a significant role.

Looking at O_3 (only) measurements, high correlations were found among the three sensors that were not exposed to direct wind (i.e. either within the cover or rear-facing). Correlation coefficients between these units' measurements were higher than 0.92. The forward-facing exposed unit (F-E), on the other hand, presents different behavior, with lower correlation coefficient values to the other three sensors, at the range of 0.51 to 0.68 (Fig. 2b shows correlation for one pyramid

trial). The O_3 measured values as a function of wind speed are presented in Fig. 4a.

The effect of velocity on the measurements is shown through the mean ratio of covered and exposed units' measurements per velocity. This was calculated by first finding the distinct ratio between each pair of samples, and then averaging all pairs for a given velocity. Fig. 4b and c show these results, per wind unit, for two sensor pairs — forward-facing, exposed (F-E), divided by either the rear-facing exposed (B-E) or the front-facing covered (F-C). For both cases, a clear trend is visible — as the wind velocity increases, the ratio increases. Thus, the forward-facing sensor, impacted by the airflow, is reporting higher concentrations of O_3. Linear regression analysis showed high correlation between the observed ratios and wind velocities of $R^2 = 0.85$ and $R^2 = 0.88$ for F-E/B-E and F-E/F-C respectively and the calculated model was proven significant with $p \ll 0.0001$ for all cases.

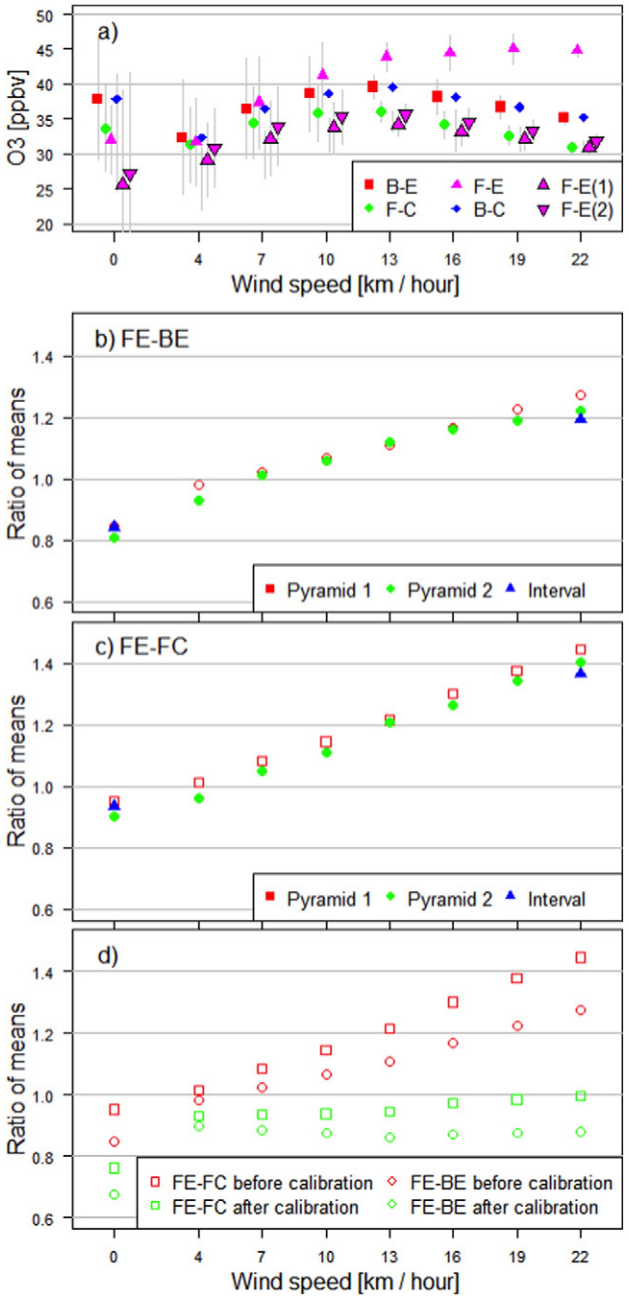

Fig. 4. O_3 wind tunnel measurements. (a) O_3 measured levels; and (b) F-E/B-E and (c) F-E/F-C ratios; (d) F-E/B-E and F-E/F-C before calibration (red squares and circles, respectively) and after (green, squares and circles correspondingly).

3.1.1. Laboratory calibration of O_3 sensors under ego-motion conditions

The ratio of measured values acquired by an exposed sensor (F-E) vs. a shielded one (F-C) are linearly correlated and can be described by the following relationship,

$$\frac{E_t}{C_t} = a \cdot v_t + b. \quad (1)$$

Where E_t and C_t are the measurements taken by exposed and covered sensors, respectively at time t, a and b are the regression parameters (slope and intercept, respectively), and v_t is the velocity in which measurements E_t and C_t were taken.

Eq. (2) shows an alternative representation of the same ratio:

$$\frac{E}{a \cdot v + b} = C. \quad (2)$$

When both sensors' have similar measured values, for a given velocity, the ratio E_t/C_t would be approximately 1. Based on the above equations, we can use the regression parameters to account for the speed effect and correct the traveling MSU's measurements.

The regression parameters were calculated separately for F-E vs. B-E and for F-E vs. F-C units during the laboratory trial and are detailed in Table S2. When applying the correction scheme to the measurements acquired by the F-E sensor, they are better correlated to those of the other three sensors (correlation coefficient improved from 0.51–0.68 to 0.89–0.93, Fig. 2b, F-E compared to F-E (1) and (2)), and the mean ratios are closer to 1 (Fig. 4d). This calibration procedure is suggested here as a means to correct measurements taken under ego-motion conditions.

3.2. Field campaign

Environmental variables, i.e., noise, temperature and relative humidity (RH), were measured by the Elm™ units during the field campaign. Noise and temperature were visibly affected by the units' motion. As velocity increased, a higher level of noise was measured by the moving sensor when compared to the stationary one. This is probably due to the wind blowing over the sensors' surface, creating local noise. Temperature readings were not found to be correlated with the increment of velocity, however in nearly *all* (>99%, *p value* <0.001) measurements pairs (stationary vs. mobile), the moving sensor measured lower temperatures than the stationary. This phenomenon is consistent with the results obtained at the laboratory experiment. RH measurements did not show any consistent behavior with respect to the sensors' traveling speeds. Detailed description of the analysis' results is discussed thoroughly in Section S.4 of the supporting information.

Ozone and Nitrogen Dioxide measurements made by sensors facing perpendicular to the car's traveling direction showed no coherent effect of the vehicle speed. Sensors facing the travel direction did show correlation with speed with a four-to-fifteen-fold and up to 60-fold increase in measured values for travel speeds of over 30 km/h, when compared to those lower than 15 km/h for various sensor pairs (for O_3 and NO_2, respectively, Figs. 5, 6a and S.5). Each point represents a single sample (1 s), taken when the moving vehicle passed along the stationary vehicle. A similar phenomenon was observed for NO_2 sensors, again, only when the sensor was facing the direction of travel (i.e., the MSU was facing left, see Fig. 1a). However, when analyzing the results for NO_2, most of the measured values were under the detection limit or equaled zero (>65%, 105 samples of 161), so no analysis was possible. It also manifests in the calculated ratios (Fig. 5), where most calculated ratios are smaller than 1 (>71%), due to the mobile sensor measuring an

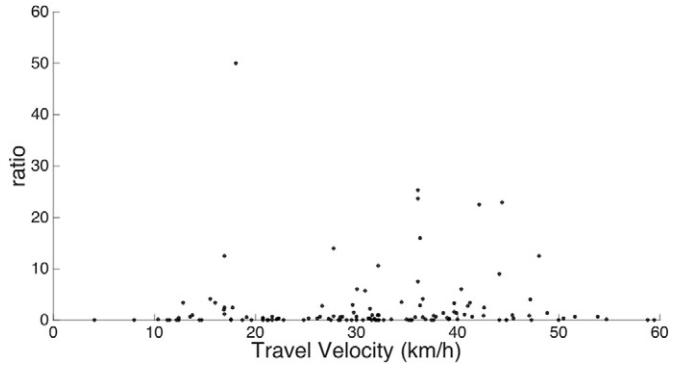

Fig. 5. NO_2 levels ratios vs. speed for all sensor pairs, during field campaign.

extremely low value. This is probably due to the same behavior we observed at the laboratory trial, that when the airflow increased, the NO_2 sensors measured very low concentrations, around and under the detection limit of 10 ppb. Thus, only partial NO_2 results were obtained, not sufficient for further discussion.

To explain the results obtained for Ozone, environmental and meteorological variables were examined. To this end, the effect of time of day, direct sunlight exposure (assessed using the images of the onboard camera), wind speed and direction (measured by a neighboring AQM station) and traffic conditions on sensors' measurements were evaluated. Only the latter showed a statistically significant effect on O_3. Wind speed and direction varied throughout the day and found not to affect the measurements of the mobile vs. stationary MSU in a significant manner. This was most likely due to the fact that both cars are facing the same direction and in the same location (about 50–100 cm apart), so they experience the same ambient wind conditions.

The increase in O_3 ratios with speed was not linear nor uniform; however, two different regimes were visible — one ranging from low to medium velocities (up to 30–35 km/h) with high ratio values (up to 12 times higher in the moving vehicle), while the other regime consisted of measurements taken while moving faster, up to 60 km/h, but the maximum ratios calculated at nearly maximum velocity were only 6 times higher in the moving vehicle compared to the stationary one (Fig. 6; (a) showing data as one series, while (b) is divided by traffic condition).

Fig. 7a and b show the O_3 ratios between units F-2 (mobile) and F-1 (stationary), presented in Fig. 6a, separated into two classes, each characterized by different traffic conditions in which the sample was acquired (Figs. 6b and S.5). When vehicle *N* is relatively close ($d < 15$ m) to the sensing vehicle, *M* (i.e. configurations 1 and 2; Fig. 7a), a slower speed of travel is expected, as a result of the road not being clear. On the other hand, when the road is clear (configurations 3, 4; Fig. 7b), the traveling speed is higher and the observed O_3 ratios are lower.

Vehicle exhaust consists of many pollutants, including O_3 precursors such as NO and volatile organic compounds (VOC). At the lower troposphere these precursors react to produce O_3 during the day. When looking at a larger (city-wide) scale of spatiotemporal air quality measurements, there is a negative correlation between NO_x and O_3 concentrations (Han et al., 2011). However, the levels of O_3 and NO_2 in real-time measurements (especially at a short time-span, like the pass of a

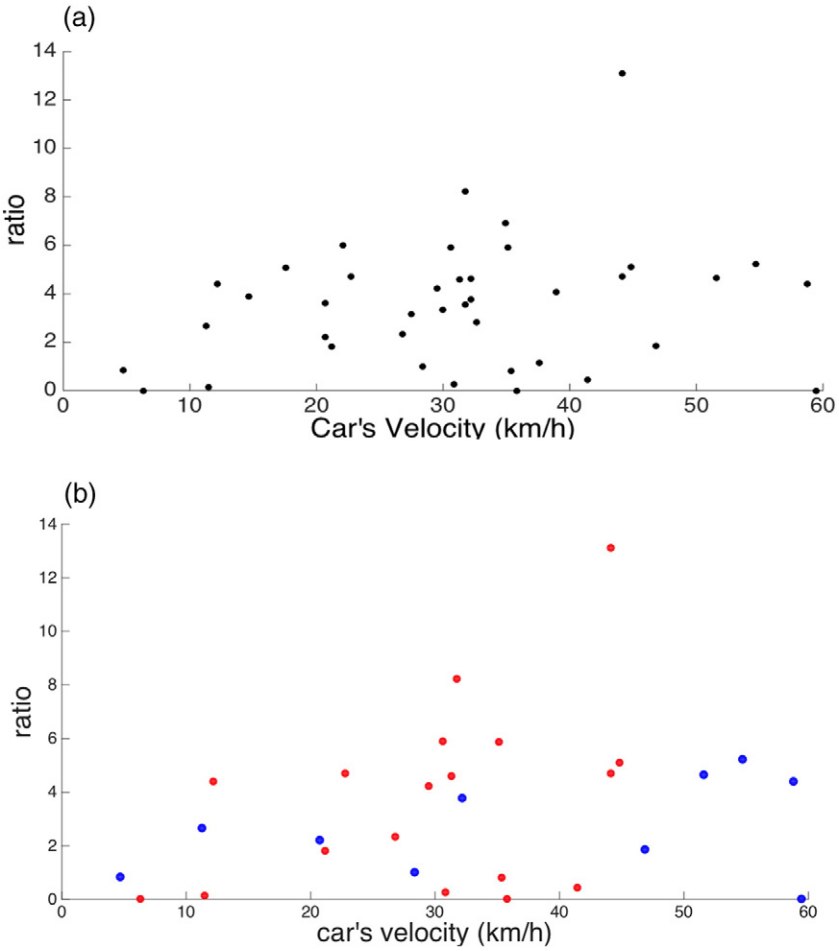

Fig. 6. O_3 levels ratios vs. speed for one sensor pair (F-2 vs. F-1), during field campaign. (a) All data as a single series; (b) data separated based on traffic conditions: red (congested road, configurations 1,2) and blue (free flow, configurations 3,4).

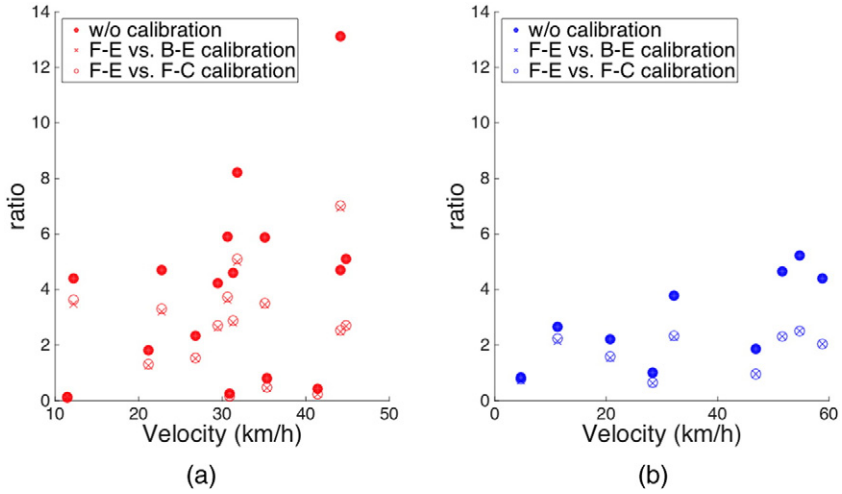

Fig. 7. O_3 levels ratios for F-2 (mobile)/F-1 (stationary) vs. speed, before (full) and after (empty) calibration for congested traffic (conditions 1 and 2) (a), and free traffic flow (conditions 3, 4) (b).

moving vehicle) at street level are part of a complex, obscure scenario (Vardoulakisa et al., 2011). Thus, there is no descriptive information of expected NO_2 and O_3 levels to be measured by our mobile MSUs at the tailpipe's level, and we have to regard only the measured results we found.

In this study, a difference was found in measured ratios depending not only on velocity, but on traffic conditions. It is assumed that when the road is denser with vehicles (slow movement with recurring acceleration/deceleration), pollution levels rise and change the ratios between different pollutants, including O_3 and its precursors. The moving unit, affected by its ego-motion as described, measures different pollutant levels when compared to the stationary one. When the traffic load is lower, the total pollutant levels also decrease and the shift caused by the sensors' miscalibration is less dominant (Fig. 7).

To further examine the general effect of car's velocity variance on the MSUs' function, standard deviation (std) was calculated for O_3 ratios, with the data divided into equivalent groups of approximately 10 km/h spans (4–15, 15–25… >55 km/h), to give 6 groups in total (Fig. 8). One sensor pair, F-2 (*M*) vs. F-3 (*S*), had very few samples taken at higher traveling speed (presented in Fig. S.5a), so the given std is less reflective of its behavior. As seen in Figs. 6 and S.5b and c (for the other three sensor pairs), the increased speed that the moving vehicle was driven increased the std for mobile vs. stationary O_3 ratios. This indicates that when the speed increases, the sensors are strongly affected and their coherence decreases. Furthermore, looking at the relative std of every sensor pair compared to the other sensors at a given speed range, it is visible that at lower speeds (4–35 km/h), the different sensor pairs' behavior resembles each other, while when increasing travel speed, it's much more diverse. This leads to the assumption that different sensor pairs may react differently to the velocity changes, i.e. the effect is not identical for all MSUs. This phenomenon should also be taken into account for mobile monitoring campaigns.

The field campaign measurements were corrected by implementing the same calibration procedure discussed above, using the regression parameters for both exposed and front-facing sensor configurations. The calibrated ratios are presented in Fig. 7a–b. As it seems, the calibration abilities are limited. There is still an increase of measurement ratios with velocity, and for all traffic conditions, the ratios are greater than 1. However, we can see that the greatest change has decreased (from fifteen to eight-fold, and from over five-fold to less than three, for both traffic configurations), and that the slope is gradual, meaning the incremental effect seen for the mobile unit is weaker post-calibration. These results show that the laboratory-based correction does decrease the influence of the sensors' ego-motion on its measurements. This correction is not perfect possibly due to many reasons such as those stated above, along with the background street conditions for example. Traffic's effect on the measurements is a contributing factor, changing the composition of pollutants in the vicinity of the sensors, which is a matter that has to be further investigated.

Future work should aim to better assess environmental traffic conditions in order to differentiate more thoroughly the various traffic configurations and validate their supporting effect for the variation in

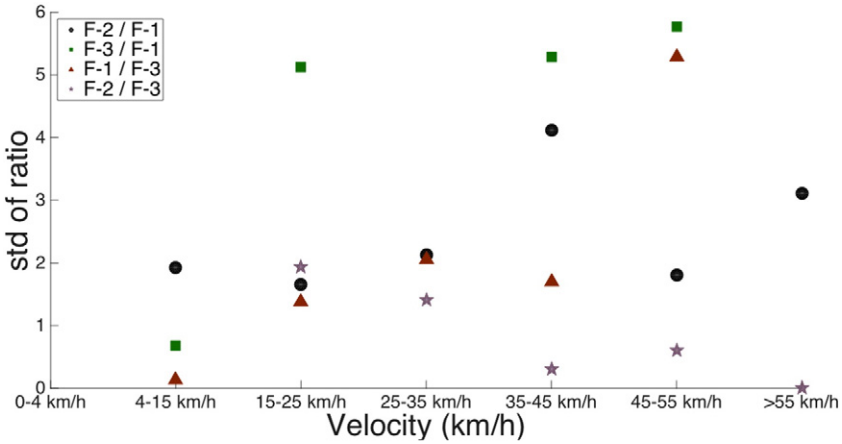

Fig. 8. Standard variation of O_3 level ratios for various sensor pairs.

measured values. Also, a laboratory-based calibration procedure should be further developed, as suggested in our work, to optimize the function based on all measurements, composing various deployment schemes. To this end, a deeper analysis has to be performed for the quantitative assessment of temperature shift of the metal-oxide sensor itself, and the resulting miscalibrated readings.

4. Conclusion

To summarize, there is a clear influence of traveling speed on almost every variable we tested for, pollutants and environmental variables as one (noise, temperature, relative humidity, O_3 and NO_2). The fact that this result was also apparent when regarding stationary, wind-exposed units, makes this behavior a very important issue since it affects every such MSU outside of laboratory conditions, mobile or stationary. Thus, it is important to account for this phenomenon when designing and deploying the units and when analyzing the results. One means of coping with this issue lies in the physical design of the MSU units by shielding the sensors from direct wind, by pre-deployment controlled trials, enabling a preliminary calibration step (similar to that which was previously suggested) but also a post-deployment correction, as demonstrated here.

MSUs offer a unique opportunity to measure pollutants immediate to the human breathing zone, at "nose height". Thus, they present unprecedented opportunity to acquire spatiotemporally-dense pollutant measurements, which better reflect personal and population exposure than standard AQM stations (Mead et al., 2013; Williams et al., 2013; Molchanov et al., 2015). This is achievable, however, only if the MSUs measurements are accurate. Therefore ego-motion and wind speed effect, both manifest as air-flow variations, will play a major role in every study aiming at using mobile or wind-exposed small air-quality monitoring units for exposure studies.

Acknowledgments

This work was partially supported by the 7th European Framework Program (FP7) ENV.2012.6.5-1, grant agreement no. 308524 (CITI-SENSE), the Technion Center of Excellence in Exposure Science and Environmental Health (TCEEH) budget # 2018567, and the New York Metropolitan Research Fund budget # 2020306.

Appendix A. Supplementary data

Supplementary data to this article can be found online at http://dx.doi.org/10.1016/j.scitotenv.2015.06.066.

References

Al Ali, A., Zualkernan, I., Aloul, F., 2010. A mobile GPRS-sensors array for air pollution monitoring. IEEE Sensors J. 10 (10), 1666–1671.
Becker, T., Muhlberger, S., Braunmuhl, C.B.-v., Muller, G., Ziemann, T., Hechtenberg, K.V., 2000. Air pollution monitoring using tin-oxide-based micro-reactor system. Sensors Actuators B 69, 108–119.
Brauer, M., 2010. How much, how long, what, and where — air pollution exposure assessment for epidemiologic studies of respiratory disease. Proc. Am. Thorac. Soc. 7 (2), 111–115.
Crouse, D.L., Goldberg, M.S., Ross, N.A., 2009. A prediction-based approach to modelling temporal and spatial variability of traffic-related air pollution in Montreal, Canada. Atmos. Environ. 43 (32), 5075–5084.
Devarakonda, S., Sevusu, P., Liu, H., Liu, R., Iftode, L., Nath, B., 2013. Real-time air quality monitoring through mobile sensing in metropolitan areas. Proceedings of the 2nd ACM SIGKDD International Workshop on Urban Computing. ACM.
Han, S., Bian, H., Feng, Y., Liu, A., Li, X., Zeng, F., Zhang, X., 2011. Analysis of the relationship between O3, NO and NO2 in Tianjin, China. Aerosol Air Qual. Res. 11, 128–139.
Honicky, R., 2011. *Towards a Societal Scale, Mobile Sensing System*, University of California at Berkeley. Electrical Engineering and Computer Sciences (Ph.D. Thesis).
International Agency for Research on Cancer (IARC), 2013. Ambient Air Pollution. *IARC Meeting Monographs*, Lyon, France.
Junninen, H., Niska, H., Tuppurainen, K., Ruuskanen, J., Kolehmainen, M., 2004. Methods for imputation of missing values in air quality data sets. Atmos. Environ. 38 (19), 2895–2907.
Kanaroglou, P., Jerrett, M., Morrison, J., Bernardo Beckerman, M., Arain, A., Gilbert, N., Brook, J., 2005. Establishing an air pollution monitoring network for intra-urban population exposure assessment: a location-allocation approach. Atmos. Environ. 39 (13), 2399–2409.
Karr, C., Rudra, C., Miller, K., Gould, T., Larson, T., Sathyanarayana, S., Koenig, J., 2009. Infant exposure to fine particulate matter and traffic and risk of hospitalization for RSV bronchiolitis in a region with lower ambient air pollution. Environ. Res. 109 (3), 321–327.
Lee, D., Lee, D., 2001. Environmental gas sensors. IEEE Sensors J. 1 (3), 214–224.
Levy, I., Mihele, C., Lu, G., Narayan, J., Hilker, N., Brook, J., 2014. Elucidating multipollutant exposure across a complex metropolitan area by systematic deployment of a mobile laboratory. Atmos. Chem. Phys. 14 (14), 7173–7193.
Levy, I., Levin, N., Yuval, Schwartz, J.D., Kark, J.D., 2015. Back-extrapolating a land use regression model for estimating past exposures to traffic-related air pollution. Environ. Sci. Technol. 49 (6), 3603–3610.
Mead, M., Popoola, O., Stewart, G., Landshoff, P., Calleja, M., Hayes, M., Baldovi, J., McLeod, M., Hodgson, T., Dicks, J., Lewis, A., Cohen, J., Baron, R., Saffell, J., Jones, R., 2013. The use of electrochemical sensors for monitoring urban air quality in low-cost, high-density networks. Atmos. Environ. 70, 186–203.
Molchanov, S., Levy, I., Etzion, Y., Lerner, U., Broday, D.M., Fishbain, B., 2015. On the feasibility of measuring urban air pollution by wireless distributed sensor networks. Sci. Total Environ. 502, 537–547.
PerkinElmer, r. "Elm Air Quality Sensor," Perkinelmer, [Online]. Available, http://elm.perkinelmer.com/ (Accessed 11 2014).
Piedrahita, R., Xiang, Y., Masson, N., Ortega, J., Collier, A., Jiang, Y., Li, K., Dick, R., Lv, Q., Hannigan, M., Shang, L., 2014. The next generation of low-cost personal air quality sensors for quantitative exposure monitoring. Atmos. Meas. Tech. 7, 3325–3336.
Pope, C.A., Burnett, R.T., Thun, M.J., Calle, E.E., Krewski, D., Ito, K., Thurston, G.D., 2002. Lung cancer, cardiopulmonary mortality, and long-term exposure to fine particulate air pollution. JAMA 287 (9), 1132–1141.
Rao, S., Chirkov, V., Dentener, F., Dingenen, R., Pachauri, S., Purohit, P., Amann, M., Heyes, C., Kinney, P., Kolp, P.K.Z., Riahi, K., Schoepp, W., 2012. Environmental modeling and methods for estimation of the global health impacts of air pollution. Environ. Model. Assess. 17 (6), 613–622.
Snedecor, G.W., Cochran, W.G., 1989. Statistical Methods. 8th ed. Iowa State University Press, Ames, Iowa, USA.
Spinelle, L., Aleixandre, M., Gerboles, M., 2013. Protocol of evaluation and calibration of low-cost gas sensors for the monitoring of air pollution. European Commission Joint Research Centre, Institute for Environment and Sustainability. European Union, Luxembourg.
Tsujita, W., Yoshino, A., Ishida, H., Moriizumi, T., 2005. Gas sensor network for air-pollution monitoring. Sensors Actuators B 110, 304–311.
Vardoulakisa, S., Solazzo, E., Lumbrerasc, J., 2011. Intra-urban and street scale variability of BTEX, NO2 and O3 in Birmingham, UK: implications for exposure assessment. Atmos. Environ. 45 (29), 5069–5078.
Wang, C., Yin, L., Zhang, L., Xiang, D., Gao, R., 2010. Metal oxide gas sensors: sensitivity and influencing factors. IEEE Sensors J. 10, 2088–2106.
Whitworth, K., Symanski, E., Lai, D., Coker, A., 2011. Kriged and modeled ambient air levels of benzene in an urban environment: an exposure assessment study. Environ. Heal. 10, 21–30.
Williams, D., Henshaw, G., Bart, M., Laing, G., Wagner, J., Naisbitt, S., Salmond, J., 2013. Validation of low-cost ozone measurement instruments suitable for use in an air-quality monitoring network. Meas. Sci. Technol. 24 (6), 5803–5814.
Wooten, R., 2011. Statistical analysis of the relationship between wind speed, pressure and temperature. J. Appl. Sci. 11, 2712–2722.